U-Pb geochronologic data from samples collected as part of the Southern Nicola Arc Project

Mitchell G. Mihalynuk
Richard M. Friedman
Corey Wall

BRITISH COLUMBIA
Ministry of Mining and Critical Minerals

GeoFile 2025-15

Ministry of Mining and Critical Minerals
Responsible Mining and Competitiveness Division
British Columbia Geological Survey

Recommended citation: Mihalynuk, M.G., Friedman, R.M., and Wall, C., 2025. U-Pb geochronologic data from samples collected as part of the Southern Nicola Arc Project. British Columbia Ministry of Mining and Critical Minerals, British Columbia Geological Survey, GeoFile 2025-15, 7p.

Front cover:
Typical dry, open interior forest, and subdued topography of south-central British Columbia where underlain by rocks of the southern Nicola arc. **Photo by Mitch Mihalynuk.**

Back cover:
Larry Diakow (right) and Yao Cui (left) were major contributors to the Southern Nicola Arc Project and aided in collection of the samples analyzed and presented here. **Photo by Mitch Mihalynuk.**

BRITISH COLUMBIA | Ministry of Mining and Critical Minerals

U-Pb geochronologic data from samples collected as part of the Southern Nicola Arc Project

Mitchell G. Mihalynuk
Richard M. Friedman
Corey Wall

Ministry of Mining and Critical Minerals
British Columbia Geological Survey
GeoFile 2025-15

U-Pb geochronologic data from samples collected as part of the Southern Nicola Arc Project

Mitchell G. Mihalynuk[1a], Richard M. Friedman[2*], and Corey Wall[2]

[1a] British Columbia Geological Survey, Ministry of Mining and Critical Minerals, Victoria, BC, V8W 9N3, Canada
[2] Pacific Centre for Isotopic and Geochemical Research, Department of Earth, Ocean and Atmospheric Sciences, University of British Columbia, Vancouver, BC, V6T 1Z4
[*] retired
[a] corresponding author: Mitch.Mihalynuk@gov.bc.ca

Recommended citation: Mihalynuk, M.G., Friedman, R.M., and Wall, C., 2025. U-Pb geochronologic data from samples collected as part of the Southern Nicola Arc Project. British Columbia Ministry of Mining and Critical Minerals, British Columbia Geological Survey, GeoFile 2025-15, 7p.

Abstract

Geofile 2025-15 contains data that support geochronological studies of the Nicola Group in southern British Columbia. This data release is focussed on methodology, quality control data, and results of U-Pb geochronological analyses of samples collected from the Nicola Group during fieldwork conducted as part of the Southern Nicola Arc Project. Here, we present one set of unpublished CA-TIMS U-Pb zircon age data, as well as data that augment those presented in Mihalynuk et al. (2025), and provide data and plots for maximum depositional age (MDA) determinations for a set of samples previously published only in graphical form.

Keywords: U-Pb geochronology, detrital zircons, Nicola Group, Quesnel terrane, Norian, Triassic-Jurassic boundary, Elkhart formation, Shrimpton formation, Copper Mountain suite, Merritt, Princeton, volcanic arc, porphyry copper mineralization

1. Introduction

Geofile 2025-15 contains data that support geochronological studies of the Nicola Group in southern British Columbia (Fig. 1). This data release is primarily focussed on methodology, quality control data, and results of U-Pb geochronological analyses of samples collected from the Nicola Group during fieldwork conducted as part of the Southern Nicola Arc Project (SNAP, Mihalynuk and Logan 2013a, b; Mihalynuk et al., 2014a, b, c; Mihalynuk et al., 2015a, b; Mihalynuk et al., 2016; Mihalynuk and Diakow, 2020; Friedman et al., 2016, 2020; Fig.2). In a companion release (Gabites and Mihalynuk, 2025), $^{40}Ar/^{39}Ar$ cooling data are presented. Here, we present data that augment the CA-TIMS U-Pb zircon analyses presented in Mihalynuk et al. (2025) and provide data and plots for maximum depositional age (MDA) determinations for a set of samples previously published only in graphical form (Mihalynuk and Diakow, 2020; shown as '(12) SNAP, unpublished data' in their Figure 4). These low precision MDAs were obtained using laser ablation inductively coupled mass spectroscopy (LA-ICP-MS) analyses on a random population of detrital zircons.

SNAP focussed on systematic quadrangle mapping of ~1000km^2 each year centered on the Summers Creek (2013), and Shrimpton Creek (2014) areas between Princeton and Merritt (Fig. 2; Mihalynuk et al., 2014c; 2015a, 2016) and some of the material presented in those reports is paraphrased here for context. Symbolic representations of the data included in this report are presented in the map and figures of Mihalynuk and Diakow (2020) along with stratigraphic data and geochronological data ready for publication at that time. The Mihalynuk and Diakow (2020) release represents the most up-to-date regional geological context for the data presented here; although some fine-tuning of age data is presented in Mihalynuk et al., (2025) where precise time of deposition (TOD) was determined for key stratigraphic intervals that were only loosely constrained by MDAs. TOD determinations used chemical abrasion-thermal ionization mass spectroscopic (CA-TIMS) analyses on a subset of young grains identified by a precursor LA-ICP-MS runs. Aided by the TOD ages, a four-stage history of Nicola arc growth can be refined: 1) 239-227 Ma, Missezula formation, arc inception and early growth, characterized by bimodal, basalt and rhyolite volcanism; 2) 227-223 Ma, Iron Mountain formation, rapid, voluminous submarine volcanic edifice growth characterized by augite-phyric basalt breccia and flows, which is locally capped by the emergent, lithologically variable Selish formation; 3) 222-210 Ma, Elkhart formation, arc extension and denudation, characterized by unconformities, oxidized conglomerate facies and interlayered hornblende-phyric basaltic flows (new TOD at base); and 4) 210-201 Ma, Shrimpton formation, arc disruption and contrasting magmatism yielding widespread biotite and apatite-phyric pyroclastics and coeval alkalic, analcime basalt flows (new TOD). Regionally important porphyry copper mineralizing processes continued until late in the latter stage, when waning arc magmatism and submergence led to deposition of overlying, increasingly finer grained sediments and thin tuffaceous layers (new TOD). A province-wide overview of

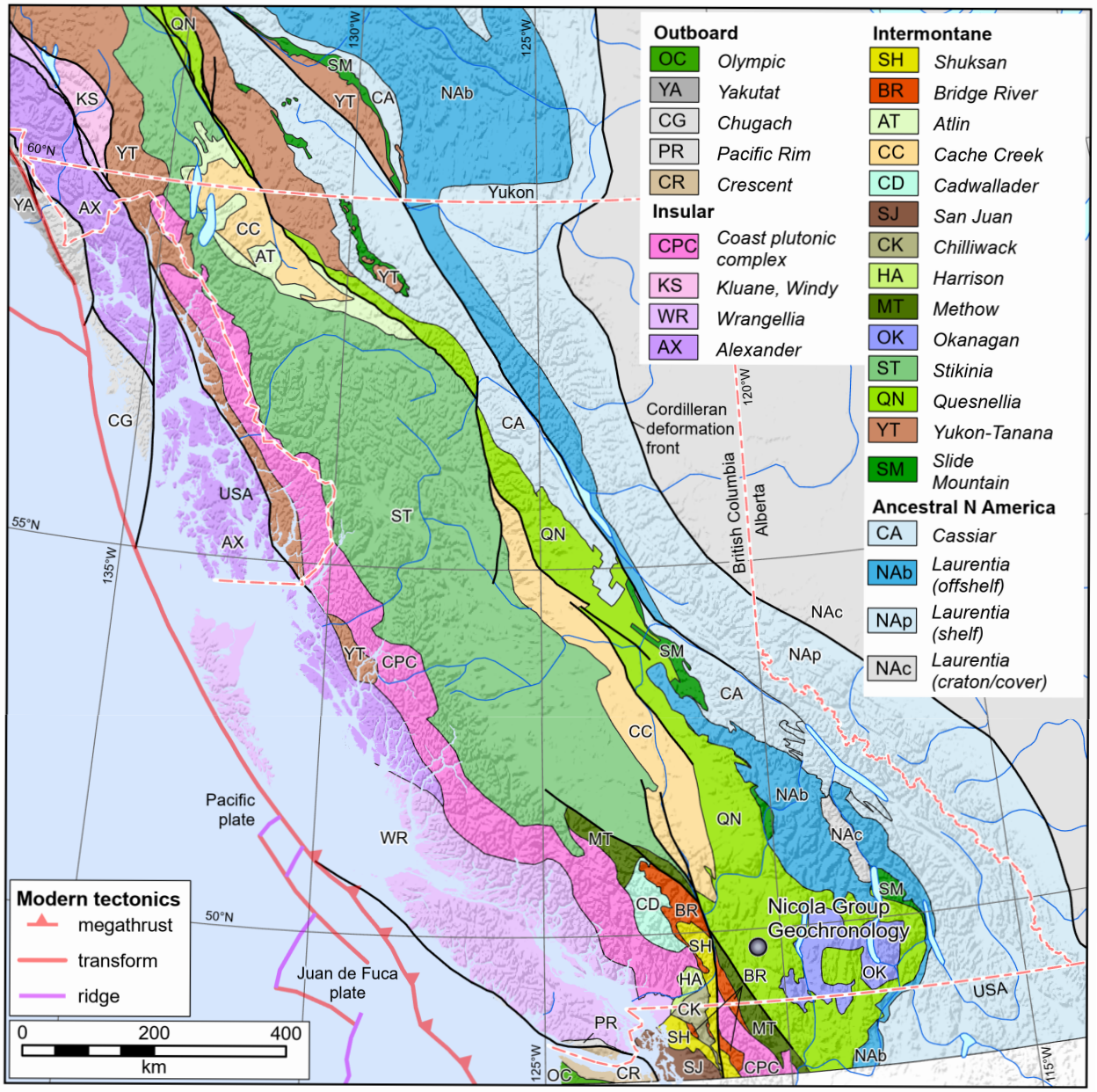

Fig. 1. Location, within the Quesnel terrane of southern British Columbia, of the Southern Nicola Arc Project and samples from which the geochronology data reported here were obtained. Terrane map adapted from Wheeler et al., (1991), Colpron and Nelson (2011), and Zagorevski et al. (2021).

the Late Triassic porphyry copper deposit epoch is presented in Logan and Mihalynuk (2014).

In the data release (BCGS_GF2025-15.zip): Appendix 1 is a folder containing cathodoluminescence (CL) imagery of sample LDi14-60-3; Appendix 2 is an Excel file with isotopic data for sample LDi14-60-3; Appendix 3 is a jpg file of CL images of sample MMI 17-8-3; Appendix 4 is jpg file of CL images of sample MMI 17-9-3; Appendix 5 is an Excel file with U-Pb zircon isotopic data and trace element data for samples MMI 17-8-3 and 17-9-3; Appendix 6 is jpg file of CL images of sample MMI 18-2-13; Appendix 7 is an Excel file with U-Pb zircon isotopic data and trace element data for sample MMI 18-2-13; and Appendix 8 is an Excel file with U-Pb zircon isotopic data and a transmitted light image of zircons in sample MMI 17-9-5 analyzed by CA-TIMS. Information in Appendices 3, 4, 5, and 8 were reported as 'unpublished' in Mihalynuk and Diakow (2020) from samples MMI 17-8-3, MMI 17-9-3, and MMI 17-9-5.

2. Methods

2.1. LA-ICP-MS analyses

Our set-up for LA-ICP-MS work followed the methods in Friedman et al. (2020). After rock samples underwent standard mineral separation procedures, zircons were handpicked in alcohol and mounted in epoxy, along with reference materials. Grain mounts were then wet ground with carbide abrasive

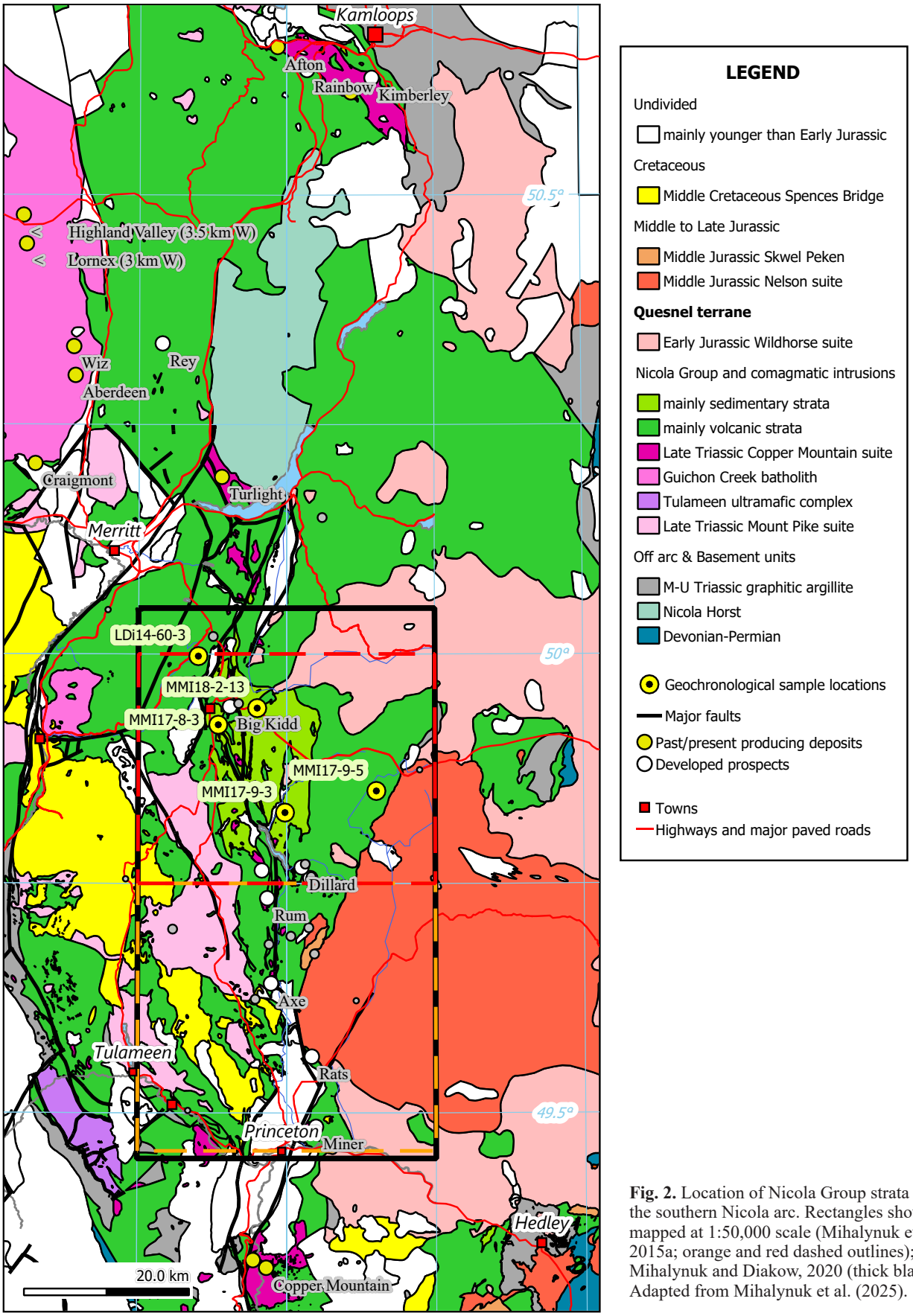

Fig. 2. Location of Nicola Group strata within the southern Nicola arc. Rectangles show areas mapped at 1:50,000 scale (Mihalynuk et al., 2014a, 2015a; orange and red dashed outlines); updated in Mihalynuk and Diakow, 2020 (thick black outline). Adapted from Mihalynuk et al. (2025).

paper and polished with diamond paste. Next, CL imaging was carried out on a Philips XL-30 scanning electron microscope (SEM) equipped with a Bruker Quanta 200 energy-dispersion X-ray microanalysis system at the Electron Microbeam/XRay Diffraction Facility (EMXDF) at the University of British Columbia. An operating voltage of 15 kV was used, with a spot diameter of 6 µm in automated CL mode, and a peak count time of 17-27 seconds. After removal of the carbon coat, the grain mount surface was washed with mild soap and rinsed with high-purity water. Before analysis, the grain mount surface was cleaned with 3 N HNO_3 acid and again rinsed with high-purity water to remove any surficial Pb contamination that could interfere with the early portions of the spot analyses.

Analyses were conducted using a Resonetics RESOlution M-50-LR, which contains a Class I laser device equipped with a UV excimer laser source (Coherent COMPex Pro 110, 193 nm, pulse width of 4 ns) and a two-volume cell designed and developed by Laurin Technic Pty. Ltd. (Australia). This sample chamber allowed for the investigation of several grain mounts in one analytical session. The laser path was fluxed by N_2 to ensure better stability. Ablation was carried out in a cell with a volume of approximately 20 cm^3 and a He gas stream that ensured better signal stability and lower U-Pb fractionation (Eggins et al., 1998). The laser cell was connected via a Teflon squid to an Agilent 7700x quadrupole ICP-MS housed at the Pacific Centre for Isotopic and Geochemical Research. A pre-ablation shot was used to ensure that the spot area on the grain surface was contamination-free. Samples and reference materials were analyzed for 36 isotopes: ^{7}Li, ^{29}Si, ^{31}P, ^{43}Ca, ^{45}Sc, ^{49}Ti, Fe (^{56}Fe, ^{57}Fe), ^{89}Y, ^{91}Zr, ^{93}Nb, ^{95}Mo, ^{98}Mo, ^{139}La, ^{140}Ce, ^{141}Pr, ^{146}Nd, ^{147}Sm, ^{153}Eu, ^{157}Gd, ^{159}Tb, ^{163}Dy, ^{165}Ho, ^{166}Er, ^{169}Tm, ^{172}Lu, ^{177}Hf, ^{181}Ta, ^{202}Hg, Pb (^{204}Pb, ^{206}Pb, ^{207}Pb, ^{208}Pb), ^{232}Th, and U (^{235}U, ^{238}U) with a dwell time of 0.02 seconds for each isotope. Pb/U and Pb/Pb ratios were determined on the same spots along with trace element concentrations. These isotopes were selected based on their relatively high natural abundances and absence of interferences. The settings for the laser were: spot size of 34 µm with a total ablation time of 30 seconds, frequency of 5 Hz, fluence of 5 J/cm^2 , power of 7.8 mJ after attenuation, pit depths of approximately 15 µm, He flow rate of 800 ml/min, N_2 flow rate of 2 ml/min, and a carrier gas (Ar) flow rate of 0.57 l/min. Reference materials were analyzed throughout the sequence to allow for drift correction and to characterize downhole fractionation for Pb/U and Pb/Pb isotopic ratios. For trace elements, NIST 612 glass was used for both drift correction and trace element calibration, with sample spacing between every five to eight unknowns, and ^{90}Zr was used as the internal standard assuming stoichiometric values for zircon. NIST 610 glass was analyzed after each NIST 612 analysis and used as a monitor reference material for trace elements. For U-Pb analyses, natural zircon reference materials were used, including Plešovice (Sláma et al., 2008; 337.13 ± 0.33 Ma) or 91500 (Wiedenbeck et al., 1995; ^{207}Pb/^{206}Pb: 1065.4 ±0.3 Ma; ^{206}Pb/^{238}U 1062.4 ±0.4 Ma) as the internal reference material and both Temora2 (Black et al. 2004; 416.78 ± 0.33 Ma) and Plešovice and/ or 91500 as monitoring reference materials; the zircon reference materials were placed between the unknowns in a similar fashion as the NIST glasses. Raw data were reduced using the Iolite 3.4 extension (Paton et al., 2011) for Igor ProTM, yielding concentration values, Pb/U and Pb/Pb dates, and their respective propagated uncertainties. Final interpretation and plotting of the analytical results employed the ISOPLOT software of Ludwig (2003).

2.2. CA-TIMS analyses

U-Pb dates were obtained by the chemical abrasion isotope dilution thermal ionisation mass spectrometry (CA-ID TIMS) method, modified after Mattinson (2005), from analyses of single zircon grains. A population of the youngest grains dated by LA-ICPMS were selected based on their igneous character as indicated by cathodoluminesce imaging. Selected zircons were plucked from their mounts and transferred into 5 µL microcapsules, placed in a large-capacity Parr vessel, and partially dissolved in 120 µL of 29 M HF for 12 h at 180 or 190°C. The zircons were returned to 3 mL Teflon PFA beakers, the HF was removed, and immersed in 3.5 M HNO_3, ultrasonically cleaned for an hour, and fluxed on a hotplate at 80°C for an hour. The HNO_3 was removed, and the zircons were rinsed twice in ultrapure H_2O (MQ-H_2O) before being reloaded into the 300 µL Teflon PFA microcapsules (rinsed and fluxed in 6 M HCl during sonication and washing of the zircon) and spiked with the EARTHTIME mixed ^{233}U–^{235}U–^{205}Pb tracer solution (ET535). Zircon was dissolved in Parr vessels in 120 µL of 29 M HF with a trace of 3.5 M HNO_3 at 220°C for 48 h, dried to fluorides, and re-dissolved in 6 M HCl at 180°C overnight. Solutions were subsequently dried down and redissolved in 60 µL of 3 M HCl to convert to $PbCl_3^-$,$UO_2Cl_3^-$, and UCl_6-ions. U and Pb were separated from the zircon matrix using an HCl-based anion-exchange chromatographic procedure (Krogh, 1973). Pb was eluted with 200 µL of 6 M HCl and U with 250 µL of MQ-H_2O into the same beaker and dried with 2 µL of 0.05 N H_3PO_4.

Pb and U were loaded on a single outgassed Re filament in 5 µL of a silica gel/phosphoric acid mixture (Gerstenberger and Haase, 1997), and U and Pb isotopic measurements were made on a Nu Instruments thermal ionisation mass spectrometer equipped with high-sensitivity 10^{13} Ω resistance Faraday detectors and an ion-counting Daly detector. Pb isotopes were measured in static Faraday mode with mass 204 on the Daly detector for 200 cycles. Mass fractionation was determined using repeat measurements of standard material solution that has equal atom ^{208}Pb and ^{206}Pb and thus measures fractionation directly (0.16±0.01 % amu^{-1}; 1σ). Transitory isobaric interferences due to high-molecular-weight organics, particularly on ^{204}Pb and ^{207}Pb, disappeared within approximately 20 cycles. Uranium was analysed as UO ions in static Faraday mode on 10^{13} Ω resistors for 200 cycles and corrected for isobaric interference of ^{233}U^{18}O^{16}O on ^{235}U^{16}O^{16}O with and ^{18}O/^{16}O ratio of 0.00206. U mass fractionation was corrected using the known ^{233}U/^{235}U ratio of the tracer solution.

U-Pb dates and uncertainties were calculated using the algorithms of Schmitz and Schoene (2007); calibration of ET535 tracer solution (Condon et al., 2015) of ^{235}U/^{205}Pb = 100.233, ^{233}U/^{205}Pb = 0.99506, and ^{205}Pb/^{204}Pb = 11268; U decay constants recommended by Jaffey et al. (1971); and of ^{238}U/^{235}U = 137.818 (Hiess et al., 2012). The ^{206}Pb/^{238}U ratios and dates were corrected for initial ^{230}Th disequilibrium using DTh/U = 0.20±0.05 (1σ) and the algorithms of Crowley et al. (2007), resulting in an increase in the ^{206}Pb/^{238}U dates of ~0.09 Ma. All common Pb in analyses was attributed

to laboratory blank and subtracted based on the measured laboratory Pb isotopic composition and associated uncertainty. Common Pb amounts vary from grain to grain (e.g., as reported in the U-Pb data table, Appendix 8). U blanks are estimated at 0.013 pg. Weighted mean $^{206}Pb/^{238}U$ dates are calculated from equivalent dates (probability of fit >0.05) using Isoplot 3.0 (Ludwig, 2003).

3. Results

Below we summarize results from three samples reported on with CA-TIMS analysis in Mihalynuk et al. (2025) followed by results from two samples referred to as 'unpublished' in Mihalynuk and Diakow (2020).

3.1. Sample LDi14-60-3 (Lat. 49.99790° N, Long. -120.64900° E), time of deposition: 222.036 ± 0.086 Ma

Sample LDi14-60-3 was collected from the base of a redbed sandstone and bladed feldspar porphyry flow section in the Kane Valley. Cathodoluminescence images of zircons from this sample are presented in Appendix 1; isotopic data from LA-ICP-MS analysis in Appendix 2 yield an MDA of ca. 220 Ma. CA-TIMS analysis (Mihalynuk et al., 2025) yielded a more precise time of deposition of 222.036 ± 0.086 Ma.

3.2. Sample MMI17-9-3 (Lat. 49.82763° N, Long, -120.50219° E), time of deposition: 202.615 ± 0.088 Ma

A limestone breccia bed (up to 0.25 m thick) with a tuffaceous sandstone matrix was collected where adjacent to thin analcime basalt flows east of upper Shrimpton Creek. Cathodoluminescence images of zircons from this sample are presented in Appendix 4; trace element and isotopic data from LA-ICP-MS analysis in Appendix 5. Based on the age distribution of detrital zircons the maximum depositional age is ca. 200 Ma (Fig. 3). CA-TIMS analysis (Mihalynuk et al., 2025) yielded a more precise time of deposition of 202.615 ± 0.088 Ma. This age is interpreted to indirectly date thin analcite-bearing basalt flows interspersed locally in the Shrimpton fine clastic succession.

3.3. Sample MMI18-2-13 (Lat. 49.9412° N, Long -120.5495° E), time of deposition: 201.304 ± 0.086 Ma

This sample was collected from homogeneous ash-tuff bands in well-bedded fossil-bearing calcareous and argillaceous siltstone, interpreted to occupy a position high in the Shrimpton formation. Cathodoluminescence images of zircons from this sample are presented in Appendix 6; isotopic and trace element data from LA-ICP-MS analysis in Appendix 7 along with a MDA of 200.2 ±1.1Ma. CA-TIMS analysis (Mihalynuk et al., 2025) yielded a more precise time of deposition of 201.304 ± 0.086 Ma.

3.4. Sample MMI17-8-3 (Lat. 49.92320° N, Long. -120.61508° E) detrital zircon maximum depositional age ca. 201 Ma

This sample is of a green volcanic-derived sandstone up to 25 cm thick in intra-arc clastic rocks of the Fairweather Hills (green lahar unit 5 of Lefebure, 1976). Cathodoluminescence images of zircons from this sample are presented in Appendix 3, trace element and isotopic data from LA-ICP-MS analysis in Appendix 5. We interpret a maximum depositional age of ca. 201 Ma based on the detrital zircon age distribution (Fig. 4).

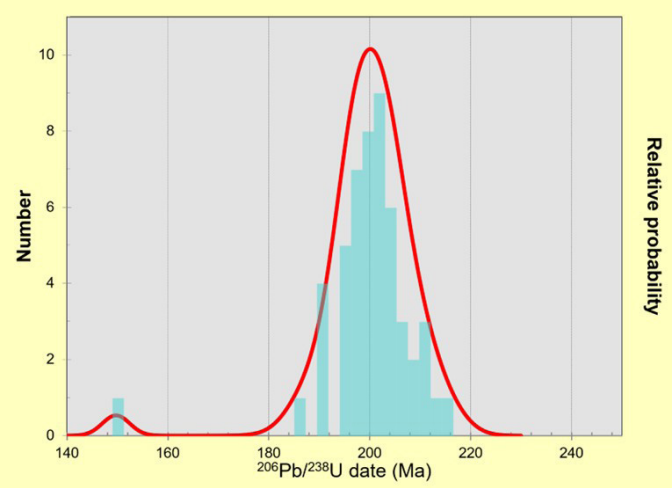

Fig. 3. Detrital zircon age distribution plot for sample MMI17-9-3. The interpreted maximum depositional age is ca. 200 Ma (confirmed by high precision TIMS analyses).

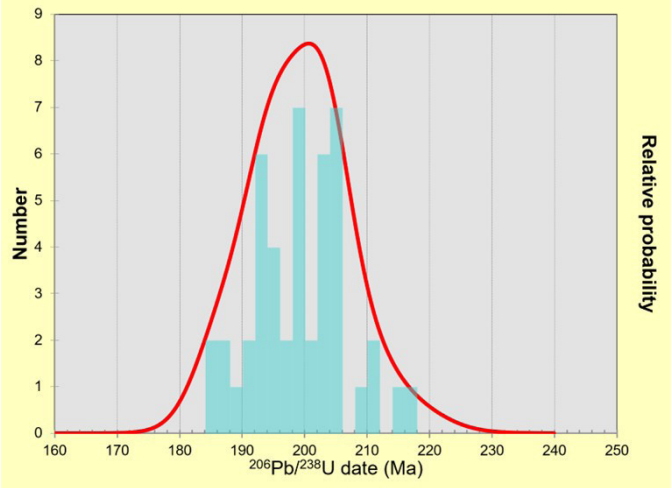

Fig. 4. Detrital zircon age distribution plot for sample MMI17-8-3. The interpreted maximum depositional age is ca. 201 Ma.

3.5. Sample MMI17-9-5 (Lat. 49.85087° N, Long -120.34889° E) age of crystallization: 222.7 ± 0.2 Ma

This sample is from a felsic lapilli and block tuff section containing local bladed basalt flows and limestone, about 5.5 km southwest of Elkhart Lake. Isotopic data and a transmitted light image of zircons analyzed by CA_TIMS are provided in Appendix 8. The best age is interpreted as 222.86 +0.23/-0.33 Ma based on the two youngest concordant CA-TIMS analyses (Fig. 5). On the basis of age and felsic composition, the unit is correlated with the Castillion member of the Selish formation.

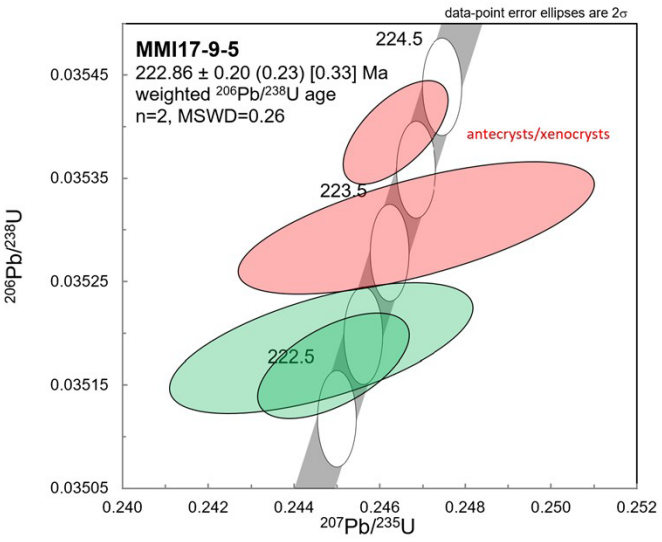

Fig. 5. Concordia plot of isotopic ratios and age determination for sample MMI17-9-5. The best age is interpreted as 222.86 +0.23/-0.33 Ma based on the two youngest concordant and overlapping determinations shown in green. Older grains shown in red are interpreted as antecrysts or xenocrysts.

References cited

Black, L.P., Kamo, S.L., Allen, C.M., Davis, D.W., Aleinikoff, J.N., Valley, J.W., Mundil, R., Campbell, I.H., Korsch, R.J, Williams, I.S., and Foudoulis, C., 2004. Improved $^{206}Pb/^{238}U$ microprobe geochronology by the monitoring of a trace-element-related matrix effect; SHRIMP, ID–TIMS, ELA–ICP–MS and oxygen isotope documentation for a series of zircon standards. Chemical Geology, 205, 115-140.

Colpron, M., and Nelson, J.L., 2011. A digital atlas of terranes for the northern Cordillera. British Columbia Ministry of Energy and Mines, British Columbia Geological Survey GeoFile 2011-11.

Condon, D.J., Schoene, B., McLean, N.M., Bowring, S.A., and Parrish, R.R., 2015. Metrology and traceability of U–Pb isotope dilution geochronology (EARTHTIME Tracer Calibration Part I). Geochimica et Cosmochimica Acta, 164, 464-480.

Crowley, J.L., Schoene, B., and Bowring, S.A., 2007. U-Pb dating of zircon in the Bishop Tuff at the millennial scale. Geology, 35, 1123-1126.

Eggins S.M., Kinsley L., and Shelley J., 1998. Deposition and element fractionation processes during atmospheric pressure laser sampling for analysis by ICP-MS. Applied Surface Science, 127, 278-286.

Friedman, R.M., Mihalynuk, M.G., Diakow, L.J., and Gabites, J.E., 2016. Southern Nicola Arc Project 2015: Geochronologic data constraining Nicola Arc history along a transect near 50°N. British Columbia Ministry of Energy and Mines, British Columbia Geological Survey GeoFile 2016-03, 19p.

Friedman, R.M., Mihalynuk, M.G., and Diakow, L.J., 2020. Geochronologic data from samples collected near Pothole Lake and Pennask Mountain (NTS 92H/15, 16) as part of the Southern Nicola Arc Project. British Columbia Ministry of Energy, and Mines and Low Carbon Innovation, British Columbia Geological Survey GeoFile 2020-12, 6p.

Gabites, J., and Mihalynuk, M.G., 2025. $^{40}Ar/^{39}Ar$ geochronologic data from samples collected as part of the Southern Nicola Arc Project. British Columbia Ministry of Mining and Critical Minerals, British Columbia Geological Survey GeoFile 2025-16, 9 p.

Gerstenberger, H., and Haase, G., 1997. A highly effective emitter substance for mass spectrometric Pb isotopic ratio determinations. Chemical Geology, 136, 309-312.

Hiess, J., Condon, D.J., McLean, N., and Noble, S.R., 2012. $^{238}U/^{235}U$ systematics in terrestrial uranium-bearing minerals. Science, 335, 1610-1614.

Jaffey, A.H., Flynn, K.F., Glendenin, L.E., Bentley, W.C., and Essling, A.M., 1971. Precision measurement of half-lives and specific activities of ^{235}U and ^{238}U. Physics Review, C4, 1889-1906.

Krogh, T.E., 1973. A low-contamination method for hydrothermal decomposition of zircon and extraction of U and Pb for isotopic age determinations, Geochimica et Cosmochimica Acta, 37, 485-494.

Lefebure, D.V., 1976. Geology of the Nicola Group in the Fairweather Hills, British Columbia. Unpublished M.Sc. thesis, Queens's University, Kingston, 179p.

Logan, J.M., and Mihalynuk, M.G., 2014. Tectonic controls on early Mesozoic paired alkaline porphyry deposit belts (Cu-Au ±Ag-Pt-Pd-Mo) within the Canadian Cordillera. Economic Geology, 109, 827-858.

Ludwig, K.R., 2003. Isoplot 3.09: A geochronological toolkit for Microsoft Excel. Berkeley Geochronology Center, Special Publication 4, Berkeley.

Mattinson, J.M., 2005. Zircon U-Pb chemical abrasion (CA-TIMS) method: combined annealing and multi-step partial dissolution analysis for improved precision and accuracy of zircon ages. Chemical Geology, 220, 47-66.

Mihalynuk, M.G., and Diakow, L.J., 2020. Southern Nicola arc geology (NTS 92H/7NE, 8NW, 9W, 10E, 15E, 16W, 92I/1SW, 2SE). British Columbia Ministry of Energy, Mines and Low Carbon Innovation, British Columbia Geological Survey Geoscience Map 2020-01, scale 1:50000, 2 sheets.

Mihalynuk, M.G., and Logan, J.M., 2013a. Geological setting of Late Triassic Cu-Au porphyry mineralization at the Dillard Creek property near Merritt. In: Geological Fieldwork 2012, British Columbia Ministry of Energy and Mines, British Columbia Geological Survey Paper 2013-1, pp. 97-114.

Mihalynuk, M.G., and Logan, J.M., 2013b. Geological setting of Late Triassic Cu-Au porphyry mineralization at Miner Mountain, Princeton southern British Columbia. In: Geological Fieldwork 2012, British Columbia Ministry of Energy and Mines, British Columbia Geological Survey Paper 2013-1, pp. 81-96.

Mihalynuk, M.G., Logan, J.M., Diakow, L.J., Henderson, M.A., Jacob, J., and Watson, A.K.G., 2014a. Summers Creek area preliminary geology (NTS 092H/9W & 10E). British Columbia Ministry of Energy and Mines, British Columbia Geological Survey Open File 2014-05.

Mihalynuk, M.G., Logan, J.M., Diakow, L.J., Friedman, R.M., and Gabities, J., 2014b. Southern Nicola Arc Project (SNAP): preliminary results. In: Geological Fieldwork 2013, British Columbia Ministry of Energy and Mines, British Columbia Geological Survey Paper 2014-1, pp. 29-57.

Mihalynuk, M.G., Friedman, R.M., Gabites, J.E., and Logan, J.M., 2014c. Southern Nicola Arc Project 2013: Geochronological data. British Columbia Ministry of Energy and Mines, British Columbia Geological Survey, GeoFile 2014-3, 7p.

Mihalynuk, M.G., Diakow, L.J., Logan, J.M., and Friedman, R.M., 2015a. Preliminary geology of the Shrimpton Creek area (NTS 092H/15E, 16W) Southern Nicola Arc Project. In: Geological Fieldwork 2014, British Columbia Ministry of Energy and Mines, British Columbia Geological Survey Paper 2015-1, pp. 129-163.

Mihalynuk, M.G., Friedman, R.M., and Logan, J.M., 2015b. Southern Nicola Arc Project 2014: Geochronological data. British Columbia Ministry of Energy and Mines, British Columbia Geological Survey, GeoFile 2015-02, 7p.

Mihalynuk, M.G., Diakow, L.J., Friedman, R.M., and Logan, J.M., 2016. Chronology of southern Nicola arc stratigraphy and deformation. In: Geological Fieldwork 2015, British Columbia Ministry of Energy and Mines, British Columbia Geological Survey Paper 2016-1, pp. 31-63.

Patton, C., Hellstrom, J., Paul, B., Woodhead, J., and Hergt, J., 2011. Iolite: freeware for the visualization and processing of mass spectrometry data. Journal of Analytical Atomic Spectroscopy, 26, 2508-2518.

Schmitz, M.D., and Schoene, B., 2007. Derivation of isotope ratios, errors, and error correlations for U-Pb geochronology using ^{205}Pb-^{235}U(^{233}U)-spiked isotope dilution thermal ionization mass spectrometric data. Geochemistry, Geophysics, Geosystems, 8. https://agupubs.onlinelibrary.wiley.com/doi/pdf/10.1029/2006GC001492

Sláma, J., Kosler, J., Condon, D.J., Crowlley, J.L., Gerdes, A., Hanchar, J.M., Horstwood, M.S.A., Morris, G.A., Nasdala, L., Norberg, N., Schaltegger, U., Xchoene, B., Tubrett, M.N., and Whitehouse, M. J., 2008. Plesovice zircon – A new natural reference material for U-Pb and Hf isotopic microanalysis. Chemical Geology, 249, 1-35.

Wiedenbeck, M., Alle, P., Corfu, F., Griffin, W.L., Meier, M., Oberli, F., Quadt, A.V., Roddick, J.C., and Spiegel, W., 1995. Three natural zircon standards for U-Th-Pb, Lu-Hf, trace element and REE analyses. Geostandards Newsletter, 19, 1-23.

Wheeler, J.O., Brookfield, A.J., Gabrielse, H., Monger, J.W.H., Tipper, H.W., and Woodsworth, G.J., 1991. Terrane map of the Canadian Cordillera, Geological Survey of Canada, "A" Series Map 1713A, 2 sheets, scale 1:2000000.

Zagorevski, A., van Staal, C.R., Bédard, J.H., Bogatu, A., Canil, D., Coleman, M., Golding, M., Joyce, N.L., Lawley, C., McGoldrick, S., Mihalynuk, M.G., Milidragovic, D., Parsons, A., and Schiarizza, P., 2021. Overview of Cordilleran oceanic terranes and their significance for the tectonic evolution of the northern Cordillera. In: Ryan, J.J. and Zagorevski, A., (Eds.), Northern Cordillera geology: a synthesis of research from the Geo-mapping for Energy and Minerals program, British Columbia and Yukon. Geological Survey of Canada, Bulletin 610, pp. 21-65.

BRITISH COLUMBIA
Ministry of Mining and Critical Minerals

BRITISH COLUMBIA GEOLOGICAL SURVEY
est. 1895